Magnesium Technology 2012
Edited by: Suveen N. Mathaudhu, Wim H. Sillekens, Neale R. Neelameggham, and Norbert Hort
TMS (The Minerals, Metals & Materials Society), 2012

CORROSION OF ULTRASONIC SPOT WELDED JOINTS OF MAGNESIUM TO STEEL

Tsung-Yu Pan[1], Michael L. Santella[1]
[1]Oak Ridge National Laboratory, One Bethel Valley Road, PO Box 2008, Oak Ridge, TN 37831-6096, USA

Keywords: Magnesium, Steel, Ultrasonic Spot Welding, Galvanic Corrosion, Automotive

Abstract

Mixed-metal joining, especially between magnesium and steel, is one of the critical technologies in achieving light-weighting vehicle body construction. However, galvanic corrosion between mixed metal joints is inevitable but not well quantified. In this study, 1.6 mm thick Mg AZ31B-H24 was joined to 0.8 mm thick hot-dipped galvanized (HDG) mild steel by ultrasonic spot welding in lap-shear configuration. No specific corrosion protection was applied in order to study worst-case conditions for corrosion behavior. The approach used an automotive cyclic corrosion test - Ford Arizona Proving Ground Equivalent Corrosion Cycle (APGE), which includes cycles of dipping in a salt bath, air drying, then holding in constant humidity environment. Lap-shear strength of the joints decreased linearly with the exposure cycles. All the joints were either taken out of test cycle for mechanical test or they separated within the humidity chamber before 25th cycle. X-ray diffraction analysis confirmed the formation of $Mg(OH)_2$ deposit in the crevice between the AZ31 and steel sheets and on the surface of the AZ31. The deposit grew thicker with cycles with exerting enough force to deform the AZ31 and HDG steel and causing a gradual opening of joints. The corrosion of the AZ31 was localized and non-uniform. The most severe corrosion occurred not at the intersection of AZ31 and the steel but rather 15-20 mm away from the spot welds.

Introduction

Magnesium (Mg) has great potential for weight reduction as it is the lightest structural metal known (78% lighter than steel, and 36% lighter than aluminum), has a high specific strength and superior damping capacity [1]. Moreover, Mg is one of the most abundant elements in the earth's crust and in seawater, and it can supply industry's needs for the foreseeable future. The ability to significantly increase Mg usage will help the auto industry meet future Federal Corporate Average Fuel Economy (CAFE) targets and reduce exposure to CAFE penalties. United States Automotive Materials Partnership (USAMP) has proposed reducing the weight of an average North American vehicle (1,527 kg) by 132 kg by replacing 286 kg of current aluminum, iron, and steel with Mg [2]. As a result, the weight reduction could benefit in reducing emissions and improving fuel consumption by approximately 5% [3].

Two of the specific areas of concerns for broader use of Mg are reliable joining methods and corrosion. These two concerns are significantly magnified when dealing with Mg components attached to steel structures. The U.S. Department of Energy (DOE) has been sponsoring projects to develop solid-state joining technologies based on friction stir linear and spot welding (FSW/FSSW) and ultrasonic spot welding (USW) for joining Mg alloys to steels. Both processes have demonstrated some potential for meeting this challenge. Some of the results have been published in [4,5,6]. An additional concern for Mg-steel joints is galvanic corrosion because of the direct contact between these metals. The four items needed to initiate galvanic corrosion action are: (1) an anode (e.g. magnesium), (2) direct electrical contact, (3) a cathode (e.g. steel), and (4) the presence of electrolyte (e.g. winter road salt) at the interface between anode and cathode. All these conditions would be met for Mg-steel spot welds in an automotive corrosive environment. It was the objective in this study to evaluate the severity of galvanic corrosion of Mg-steel USW through simple observation of corrosion products and changes of joint strength. It was not the intention to study the details of corrosion mechanisms.

Experiments

Mg and Steel Specimens

The materials, machine, and fixture used to make ultrasonic spot welded lap-shear samples were identical to those described in [4,5]. The materials used for these experiments were sheets of 0.8-mm-thick hot-dip-galvanized (HDG) mild steel and 1.6-mm thick AZ31B-H24. Prior to welding the surfaces of the AZ31B sheet were buffed with non-metallic abrasive pads (Scotch-Brite™) to remove surface oxides and produce shiny surfaces. Both metals were cleaned with acetone followed by isopropyl alcohol to remove lubricants and surface debris. The coupons used for welding the lap-shear test specimens had dimensions of 100 mm × 30 mm, and they were overlapped a distance of 75 mm in a fixture. The welds were centered in the overlap region. The only clamping between the coupons was the pressure applied by the welding (sonotrode) tip. Specimens were positioned for welding so that the primary vibration direction of the sonotrode was perpendicular to their long axis.

Ultrasonic Spot Welding

The machine used for the ultrasonic spot welding was a single-transducer wedge-reed Sonobond CLF 2500. Spot welding was done using a power of 1500 W at impedance setting 6 and welding time of 1.0 sec. The sonotrode tip was made from T1 steel, and it had a flat, rectangular face of 7 mm × 7 mm as shown in [5]. The line pressure to the tip clamping mechanism was adjusted to make the welds under constant nominal pressure of 39 MPa.

Corrosion Cycling Test

An automotive corrosion cycle test was chosen. Lap-shear coupons were cycled through Ford's "Arizona Proving Ground Equivalent" (APGE) corrosion cycle [7]. The test protocol is:

Step	*Duration*	*Description*
1	15 min	Immersion in 5% NaCl solution, agitated
2	3 hours	Air dry
3	20 hr 45 min	Humidity chamber, 50°C 85% RH

Standard Ford test protocol calls for a complete test to consist of 30 cycles.

In our laboratory, the humidity chamber was a covered glass desiccator with HFP85 potassium chloride saturated aqueous salt solution in a 50°C furnace. The chamber was set up according to the practice defined in ASTM E104-02 [8], which provides ~81% relative humidity at 50°C. No potassium could be detected on exposed samples by energy dispersive spectrometry (EDS) in a scanning electron microscope (SEM).

A total of 30 samples were used for the corrosion cycle test, with an intended plan that one sample would be taken out of test every cycle between 5th and 30th cycles for mechanical lap-shear test. In addition, samples from every 5th cycle were preserved for cross-sectioning and metallographic evaluation.

Lap-shear Mechanical Test

Lap-shear joint strength was measured on an Instron machine at a crosshead speed of 10 mm/min to record the maximum failure load. There was no spacer added to offset the centerline.

X-ray Diffraction (XRD)

Oxidation residue was examined by XRD to study the compounds. Residue from AZ31 samples was ground in a mortar and pestle to a very fine size. Powder x-ray diffraction was performed to determine the composition of the residue. Vaseline was used as the binder and was spread onto a glass slide and the powder was finely dispersed onto this binder. XRD was performed from 15-90°.

Results and Discussions

Before the 25th cycle, all of the samples were either taken out of the test at specific assigned cycles for mechanical and metallographic analysis, or the joints were completely separated in the humidity chamber.

Joint Strength

The results of the lap-shear testing are presented in Figure 1 where lap-shear strength is plotted against the cycles of exposure. The average strength of non-corroded samples was 4.2 kN [6], shown as the dash baseline in comparing the strength of corroded samples. The joint strength decreases continuously and almost linearly with number of cycles. The last surviving sample was taken out after the 24th cycle and was measured with a failure load of only 0.4 kN. Several samples separated spontaneously in the humidity chamber during the test and were not able to be measured for the strength. Joints up to 17 cycles had what could be considered practically useful strength.

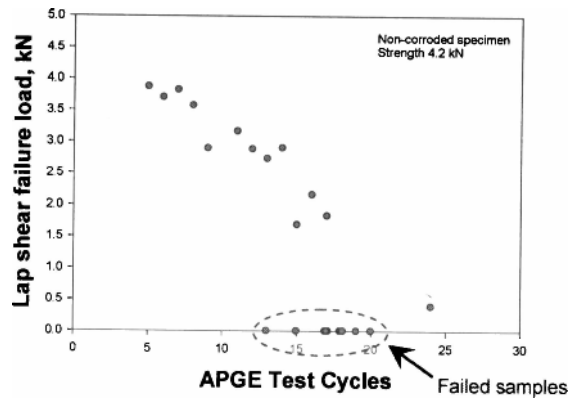

Figure 1. Lap-shear joint strength of USW Mg-steel samples after cyclic corrosion test.

Appearances of the Samples

Deposits grew immediately beginning from the 1st cycle of exposure. Figure 2 shows the appearance of the AZ31 surface where deposits appeared as discrete pits. The pattern of the pits seemed related to the texture of roughness on the surface. Such deposits continued growing in subsequent cycles. After cycle 5, deposits were so dense and thick that the USW joint was hardly visible, as shown in Figure 3. The pits are similar to the pitting corrosion of Mg in aqueous solution with chloride observed by Tunold et al. [9]. They concluded that pitting was initiated by the presence of chloride ions on the metal surface.

Figure 2. Appearance of AZ31 surface after 1 cycle of corrosion test.

Corrosion deposits also grew in the crevices between the AZ31 and steel. Figure 4 is an optical image of the side view of the sample after 5 cycles of corrosion test, clearly showing the deposit grew in-between the AZ31 and steel sheets causing a slight opening of the joint. The deposits in the crevices grew thicker with each successive cycle of exposure. Figure 5 shows a sample after 16 cycles of test. The deposit not only grew thicker, but it also caused significant bending of the steel.

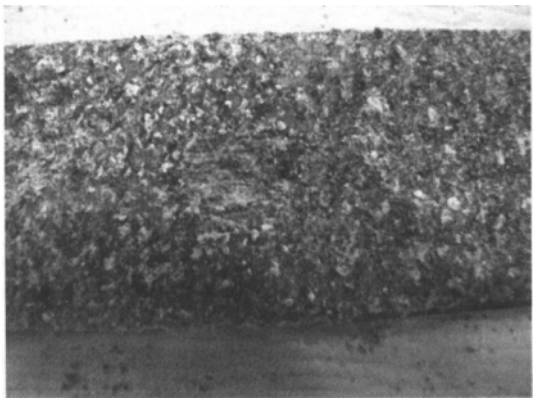

Figure 3. Appearance of AZ31 surface after 5 cycles of corrosion test.

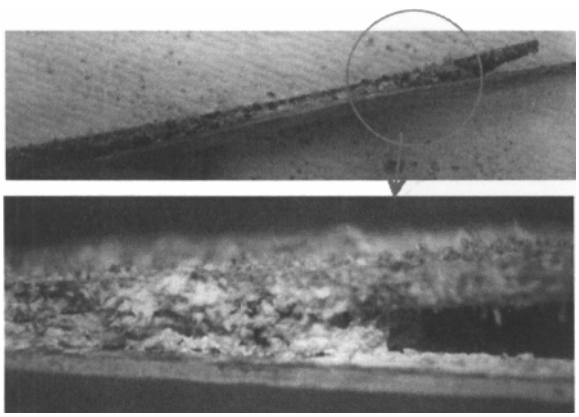

Figure 4. Oxide in the crevice between AZ31 and steel, after 5 cycles of corrosion test. AZ31 was on top.

In addition to the side view of the joint sample, the deposits in the crevices could also be seen after the joints were separated either during the corrosion test or after the mechanical lap-shear test. Figure 6 shows the image of matching (inner) surfaces of the AZ31 and steel after a sample separated after 18 cycles of corrosion test. A large white piece of deposit, about 50 mm in length and across the width of the sheet (30 mm), can be seen adhering to the AZ31. However, from sample to sample, the deposit could be attached to either AZ31 or steel when the joint was separated.

XRD and EDS Analyses

Samples of deposit were analyzed by X-ray diffraction. A representative spectrum is shown in Figure 7. Residues were identified as $Mg(OH)_2$ with major peaks matched exactly as in [10,11]. No sodium (Na) was found in the deposits.

The finding of $Mg(OH)_2$ is in agreement with other published observations [10,12,13,14]. All of those studies were conducted by immersing in aqueous NaCl solutions. It seems, however, that the NaCl immersion, drying, and cyclic exposure to 85% RH humidity produce the same basic corrosion response.

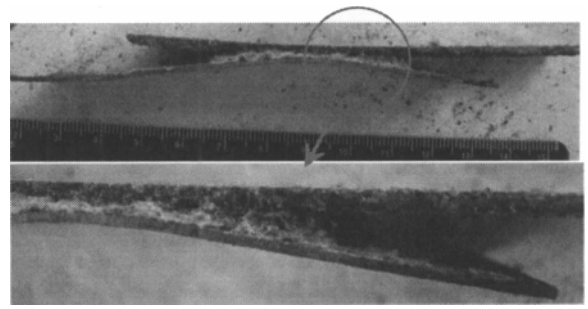

Figure 5. Oxide in the crevice between AZ31 and steel after 16 cycles of corrosion test. AZ31 was on top.

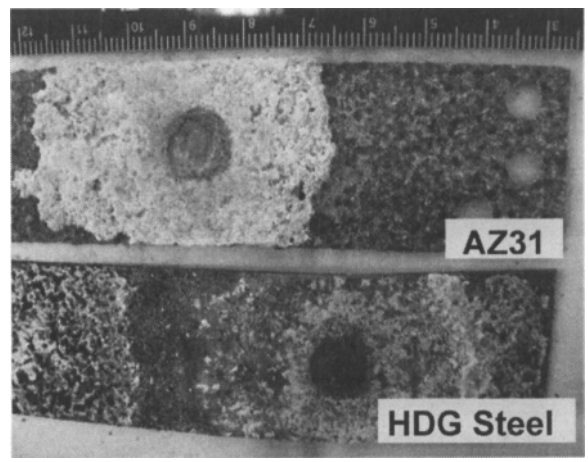

Figure 6. Appearance of the matching (inner) surfaces of AZ31 and HDG steel specimens after 18 cycles of corrosion test.

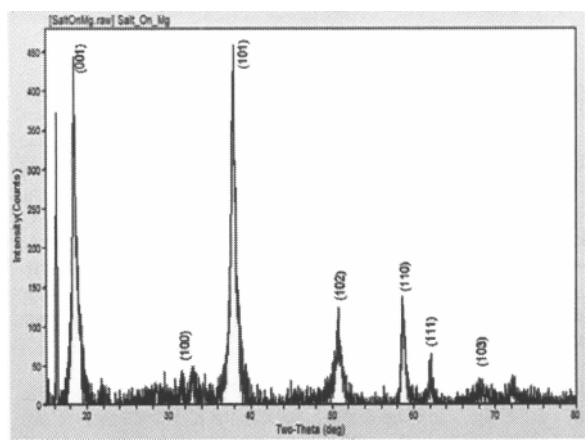

Figure 7. X-ray diffraction analysis result of the deposit.

In Figure 6, the surface of the deposit facing the steel sheet has a layer of ZnO, identified from the EDS analysis, indicating the consumption of the Zn HDG coating on the steel surface. As exposure cycles accumulated the Zn was progressively consumed. That led to exposure of fresh steel surface to the corrosive environment producing brown-color iron oxides.

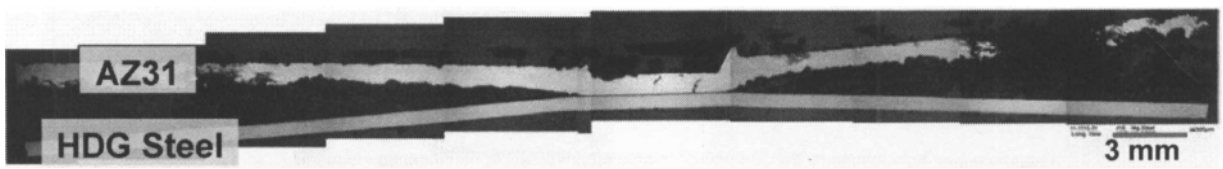

Figure 8. Optical micrograph of cross-section of a sample after 10 cycles of corrosion test. The AZ31 is on top and the HDG steel is at the bottom.

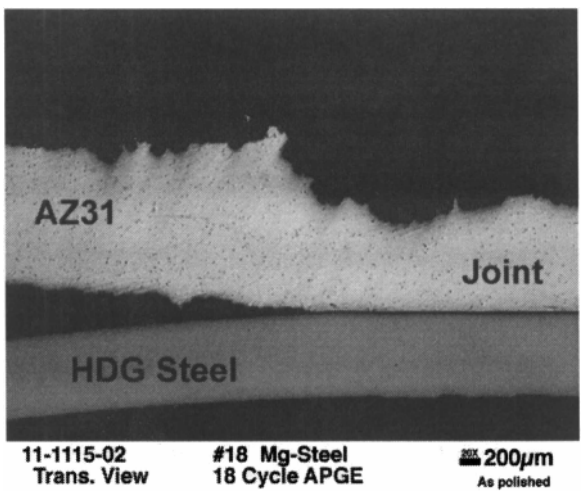

Figure 9. Optical micrograph of cross-sectioned USW after 10 cycles of corrosion test.

Cross-section Micrographs

Samples of every 5th cycle were cross-section, mounted, and polished to examine the depth of corrosion and microstructure of the AZ31. Figure 8 is a composite photo from several micrographs of the sample after 10 exposure cycles. It shows that both AZ31 and steel have been deformed, with steel being deformed more severely than the AZ31. The distance of the gap between Mg and steel was about 5 mm at a location 10 mm away from the joint. Since the original non-corroded samples had very tight fits between AZ31 and steel, the gap, which widened with cycles, was clearly opened by the force from the growth of deposit in the crevice.

Figure 9 is an optical micrograph of an area showing both the joint on the right and the crevice between AZ31 and steel on the left. The corrosion in the AZ31 proceeded by pitting and occurred on both its outer and inner surfaces, as well as into the matrix of Mg. By matching the appearance of the sample before cross-sectioning, the dark circles on top of the AZ31 surface are believed to be the $Mg(OH)_2$ deposit. Similar localized corrosion was shown by Pardo et al [12] for AZ31 immersed in 3.5% NaCl solution. It was said that the $MnAl_2$ inclusions and β-phase ($Mg_{17}Al_{12}$) formed a galvanic couple with the surrounding Mg matrix which caused localized corrosion. The front of corrosion attack was stopped when it reached the lamellar aggregate of the β-phase ($Mg_{17}Al_{12}$). The existence of localized galvanic cells certainly could explain the localized corrosion observed in this study. It may also be influenced by local microstructure, which is affected by the ultrasonic spot welding [4].

The corrosion on the AZ31 sheet was not only localized but also non-uniform across the length of the sample. It can be seen in Figure 8 that the thinning of the Mg sheet was more severe not near the joint but rather at the distance about 15 to 20 mm away from it. This may be related to the "global" galvanic couple between Mg and steel which caused the maximum corrosion to be away from the point of contact. There was no attempt in this study to analyze the detailed mechanism. However, the phenomenon is similar to what was reported in [15] where the corrosion between aluminum and a steel bolt was studied. The maximum corrosion in aluminum was found to be about 1 to 2 mm away from the aluminum-steel contact interface.

Corrosion did not occur at the welded interface between steel and AZ31. Figures 10 (a) and (b) shows the failure surfaces of AZ31 and steel sheet, respectively, following lap-shear testing sample after 14 exposure cycles. A small bump, or a nugget, can be seen on the shiny metal surface. The sample had a failure load of 2.9 kN, about 70% of the non-corroded samples (4.2kN). EDS analysis on the failure surface of this joint showed Mg on both sides of the sheets, indicating the failure occurred within the Mg material. It is also evident from Figure 9 that there was no corrosion at the welded interface.

The size of the fractured Mg interface gets smaller with the number of corrosion cycles. This would be due to the penetration of corrosive medium into the interface when the joint is gradually pushed open from the growth of the deposit in the crevice. The decrease of joint strength was due to the reduced size of the remaining welded metal.

Conclusions

The ultrasonic spot welds between AZ31B-H24 and HDG steel was evaluated after an automotive cyclic corrosion test. In order to simulate the worst corrosive situation, no protective coating or other means to minimize the galvanic corrosion was used. Joint strength decreased continuously and linearly with the cycles of corrosion from 4.2kN of non-corroded samples to complete spontaneous failure before the 25th exposure cycle. No practical joint strength was preserved after 17 cycles. Deposits of $Mg(OH)_2$, identified by X-ray diffraction, mainly grew in the crevices between the AZ31 and steel sheets, and to a much less degree, on the outer surfaces of the AZ31. Deposits grew thicker with exposure cycles, causing the deformation of the steel and AZ31 sheets.

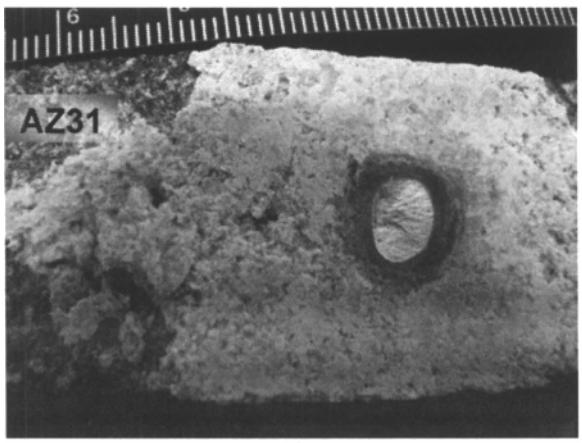

(a)

(b)

Figure 10. Failure surface of (a) AZ31 and (b) HDG steel after lap-shear test. The sample was gone through 14 cycles of corrosion tests.

Welded joint interfaces between AZ31 and steel were not directly attacked by the corrosion. But the joint area decreased from the consequence of the opening of the joint due to the growth of deposits. Metallographic study showed localized and non-uniform corrosion on Mg, with the most severe corrosion occurring somewhere about 15 to 20 mm away from the joint. Detailed mechanism was not studied but it was believed to be associated with the "global" galvanic cell between Mg and steel.

Acknowledgements

This research was sponsored by the U.S. Department of Energy, Assistant Secretary for Energy Efficiency and Renewable Energy, Office of Vehicle Technologies, as part of the Lightweight Materials Program. The authors also appreciated Ms. Katherine Strader for performing the x-ray diffraction analysis, and Dr. Robert C. McCune for his valuable suggestions and discussions for the corrosion test setup and experimental results.

References

1. R.S. Beals, C. Tissington, X. Zhang, K. Kainer, J. Petrillo, M. Verbrugge, "Magnesium global development: Outcomes from the TMS 2007 annual meeting", *JOM*, **59**(8) (2007), pp. 39–42.
2. N.N., "Magnesium Vision 2020: A North American Automotive Strategic Vision for Magnesium", United States Automotive Materials Partnership (USAMP) Automotive Metals Division (AMD), released November 2006.
3. E. Wall, R. Sullivan, J. Carpenter, "Automotive Lightweighting Materials FY 2006 Progress Report", http://www1.eere.energy.gov/vehiclesandfuels/pdfs/alm_06/2g_osborne.pdf, October 2007.
4. M.L. Santella, T.J. Franklin, J. Pan, T. Pan, E. Brown, "Ultrasonic Spot Welding of AZ31B to Galvanized Mild Steel", *SAE International Journal of Materials and Manufacturing*. **3**(1) (2010) pp. 652-657
5. T.J. Franklin, J. Pan, M.L. Santella, T. Pan, "Fatigue Behavior of Dissimilar Ultrasonic Spot Welds in Lap-Shear Specimens of Magnesium and Steel Sheets" *SAE Technical Paper* 2011-01-0475, April 2011.
6. S. Jana, Y. Hovanski, G.J. Grant. "Friction Stir Lap Welding of Magnesium Alloy to Steel: A Preliminary Investigation." *Metallurgical and Materials Transactions. A, Physical Metallurgy and Materials Science* **41A**(12) (2010) pp. 3173-3182.
7. K. Lazarz, R.C. McCune, W. Wang, P.K. Mallick, "Effect of Surface Pretreatments on Adhesive Bonding and Corrosion Resistance of AM60B, AZ31-H24, and AM30 Magnesium", *SAE Technical Paper* 2009-01-0037, April 2009.
8. N.N., "Standard Practice for Maintaining Constant Relative Humidity by Means of Aqueous Solutions", ASTM E104 – 02 (2007).
9. R. Tunold, H. Holtan, M. Hägg Berge, A. Lasson, R. Steen-Hansen, "The Corrosion Of Magnesium In Aqueous Solution Containing Chloride Ions", *Corrosion Science*, **17**(4) (1977), pp. 353-365.
10. R. Ambat, "Evaluation of Microstructural effects on corrosion behaviour of AZ91D magnesium alloy". *Corrosion Science* **42** (2000) pp. 1433–1455.
11. B. Xu, H, Deng, Y. Dai, B. Yang," Preparation of Nanoparticles of Magnesium Hydroxide from Bittern", *Transactions of Nonferrous Metals Society of China*, 17 (2007), pp s671-s674.
12. A. Pardo, M.C. Merino, A.E. Coy, R. Arrabal, F. Viejo, E. Matykina, "Corrosion Behaviour of Magnesium/Aluminium Alloys in 3.5 wt.% NaCl", *Corrosion Science* **50** (2008) pp. 823–834.
13. B.J. Schneider, R.C. McCune, M.S. Ricketts, J.A. Hines, "Examination of the Corrosion Behavior of Creep-Resistant Magnesium Alloys in an Aqueous Environment" *SAE Technical Paper* 2007-01-1023, April 2007.
14. G. Song, G. A. Atrens, "Recent Insights into the Mechanism of Magnesium Corrosion and Research Suggestions", *Advanced Engineering Materials*, **9**(3), (2007) pp. 177-183.
15. T. Mizukami, "Simulation of Galvanic Corrosion of Aluminum Materials for Vehicles", *SAE Technical Paper* 2010-01-0724, April 2010.